Supporting Information

Investigation of the correlation between phase structure and activity of Ni-Mo-O derived electrocatalysts for the hydrogen evolution reaction

Guo-Xuan Cao, Zheng-Jun Chen,* Hui Yin, Li-Yong Gan, Ming-Jie Zang, Ning Xu, and Ping Wang*

School of Materials Science and Engineering, Key Laboratory of Advanced Energy Storage Materials of Guangdong Province, South China University of Technology, Guangzhou 510641, People's Republic of China.

E-mail: mschenzhengjun@mail.scut.edu.cn
mspwang@scut.edu.cn

Experimental Section

***Chemicals and materials*:** Nickel nitrate hexahydrate ($Ni(NO_3)_2 \cdot 6H_2O$, 98%), urea ($(NH_2)_2CO$, ≥ 99.5%), ammonium molybdatetetrahydrate ($(NH_4)_6Mo_7O_{24} \cdot 4H_2O$, 99%), hydrochloric acid (HCl, 36~38%), platinum/carbon (Pt/C, 20 wt% Pt on Vulcan XC-72R), nafion solution (5 wt% in alcohol), tetrabutylammonium hexafluorophosphate (TBA-PF_6, 98%), acetonitrile (CH_3CN, 98%) and other reagents of analytical grade were all obtained from commercial sources and used without further purification. Deionized (DI) water was used throughout the experiments. The nickel foam (NF) with a purity of ≥ 99%, a thickness of 1.60 mm, an area density of about 650 $g \cdot m^{-2}$ and an average pore size of 0.25-0.80 mm was purchased from Incoatm.

***Preparation of electrode materials*:** The NF was consecutively cleaned in HCl solution (3 M), ethanol and DI water under sonication to remove nickel oxides, organics and other impurities on the surface. The DI water containing $Ni(NO_3)_2 \cdot 6H_2O$ (0.1 M), urea (0.25 M) and $(NH_4)_6Mo_7O_{24} \cdot 4H_2O$ (0.025 M) together with the cleaned NF (1×4 cm^2) were transferred into a 50 mL Teflon-lined stainless autoclave. The sealed autoclave was kept at 150 °C for 18 h. After cooling down to room temperature, the collected samples were washed thoroughly with DI water and ethanol and then dried in vacuum at 60 °C. Thus-prepared sample was subsequently annealed at different temperature (380 °C, 550 °C and 700 °C) under a flowing H_2 atmosphere for 2 h. The ramping rate was 10 °C min^{-1}. The Pt/C working electrode was prepared by a two-step process. First, Pt/C (5 mg) was dispersed in 1 mL isopropyl alcohol, followed by addition of 50 μL Nafion solution. After being sonicated for at least 30 min, 20 μL of the resulting catalyst ink was drop casted on a glassy-carbon electrode with a geometric area of 0.07 cm^2.

***Characterization*:** The phase structure, morphology and microstructure of the catalyst samples were characterized by X-ray diffraction (XRD, MiniFlex 600, Cu Kα radiation), field-emission scanning electron microscope (FE-SEM, ZEISS MERLIN) and high-resolution transmission electron microscopy (HRTEM, JEOL-2100F). The chemical states of the constituent elements of the catalyst samples were analyzed using X-ray photoelectron spectroscopy (XPS, Thermo Scientific K-ALPHA$^+$, Al Kα X-ray source). In the XPS measurements, high-resolution scans of elemental lines were recorded at 50 eV pass energy of the analyzer. All the binding energies were calibrated using the C1s peak (284.8 eV) of the adventitious carbon as an internal standard. The curve fitting was performed using XPS PEAK 4.1 software. Element analyses of the catalyst samples were conducted in an inductively coupled plasma-atomic emission spectrometry (ICP-AES, Iris Intrepid).

***Electrochemical measurements*:** Electrochemical measurements were carried out in a standard three-electrode system using a CHI 660E electrochemical workstation at ambient temperature. The electrochemical cell consists of a catalytic electrode as the working electrode, an Hg/HgO (with 1 M KOH) reference electrode and a graphite plate as the counter electrode. Potentials, measured versus Hg/HgO, were referenced to reversible hydrogen electrode (RHE) by adding a value of (0.059*pH + 0.098) V. Typically, a potential cycling in a range of 0 to −0.6 V vs RHE with a sweep rate of 100 mV s^{-1} was applied before the measurement of polarization curves. All

measurements of liner sweep voltammetry (LSV) were performed in an alkaline medium (1 M KOH) at a scan rate of 5 mV s^{-1}. All of the potentials were given with 80% iR compensation unless specifically noted. The electrochemical active surface areas (ECSA) of the catalyst samples were calculated from the double-layer capacitance (C_{dl}), which was determined from the scan-rate dependence of capacitive current in cyclic voltammetry (CV) measurements. Here, to ensure a reliable determination of the C_{dl}, the CV measurements were conducted in 0.15 M TBA-PF_6/CH_3CN solution.**1** Electrochemical impendence spectra (EIS) measurements were conducted in a PARSTAT MC 2000 electrochemical workstation. The impedance spectra were collected at the onset potential in a frequency range of 0.01 Hz to 100 kHz with an amplitude of 5 mV.

***Theoretical calculations*:** DFT calculations were conducted using the Vienna Ab-Initio Simulation Package with spin-polarized Perdew-Burke-Ernzerhof exchange correlation functional including van der Waals corrections (optB88).[2,3] The DFT+U[3] approach was applied to molybdenum centers in MoO_3 and a value of 3.5 eV was chosen for U-J parameter.[3] The MoO_3(010) (7.524 Å × 7.953 Å) surfaces were modeled by a three layer (1×2) and two bi-layer (1×1) periodic slab, corresponding to (7.524 Å × 7.953 Å) (see Figures S3a). A four-layer 3×3 lateral supercell (7.479 Å × 7.479 Å) was used to model Ni (111) (see Figure S3b) surface. Since $Ni_{10}Mo$ belongs to the same space group (Fm-3m, No. 255) to Ni (JCPDS 01-1258), the $Ni_{10}Mo$ catalyst was modeled by substituting a Ni atom in the first layer of Ni (111) by a Mo atom (see Figure S3c). In the simulations of Ni_4Mo and Ni_3Mo, the (121) and (211) surfaces were constructed, respectively, based on the experimental observations. The two surfaces were simulated by two four-layer 1×1 unit cells, corresponding to (8.858 Å × 6.715 Å) and (7.948 Å × 6.161 Å), respectively (see Figures S3d and S3e). A cutoff energy of 500 eV was used for the plane-wave expansion in all calculations.[5,6] Three Gamma-centered k-point grids, (5 × 5 × 1), (5 × 3 × 1) and (5 × 7 × 1), were used to sample the Brillouin zone for Ni(111)/$Ni_{10}Mo$(111)/MoO_3(010), and Ni_4Mo(121)/Ni_3Mo(211) surfaces, respectively. Dipole correction was also implemented with respect to MoO_3(010) surfaces.[7] The adsorption energy (ΔE) of adsorbates was defined as

$$\Delta E_{ad} = E_{X/surface} - E_X - E_{surface} \quad (1)$$

where $E_{H/surface}$, E_{H2} and $E_{surface}$ are the total energies of H adsorbed surfaces, H_2 in gas phase and clean surfaces, respectively. The associated change of Gibbs free energy of H was calculated as

$$\Delta G = \Delta E - \Delta ZPE - T\Delta S \quad (2)$$

with ΔZPE and ΔS being the differences of zero-point energy and of entropy between the adsorbed state and gas phase. The ZPE and entropies were calculated from the vibrational frequencies.[8] The weighted *d*-band center (ε_d) was determined using[9]

$$\varepsilon_{d-weighted} = \frac{\sum_M V^2 \varepsilon_d^M N^M}{\sum_M V^2 N^M} \quad (3)$$

where V^2 is the d-band coupling matrix element for the surface metal atom (V_{Mo}^2= 6.62, V_{Ni}^2= 1.16),[10] N^M is the number of M-H bonds and the ε_d is the *d*-band center of metal atom M.

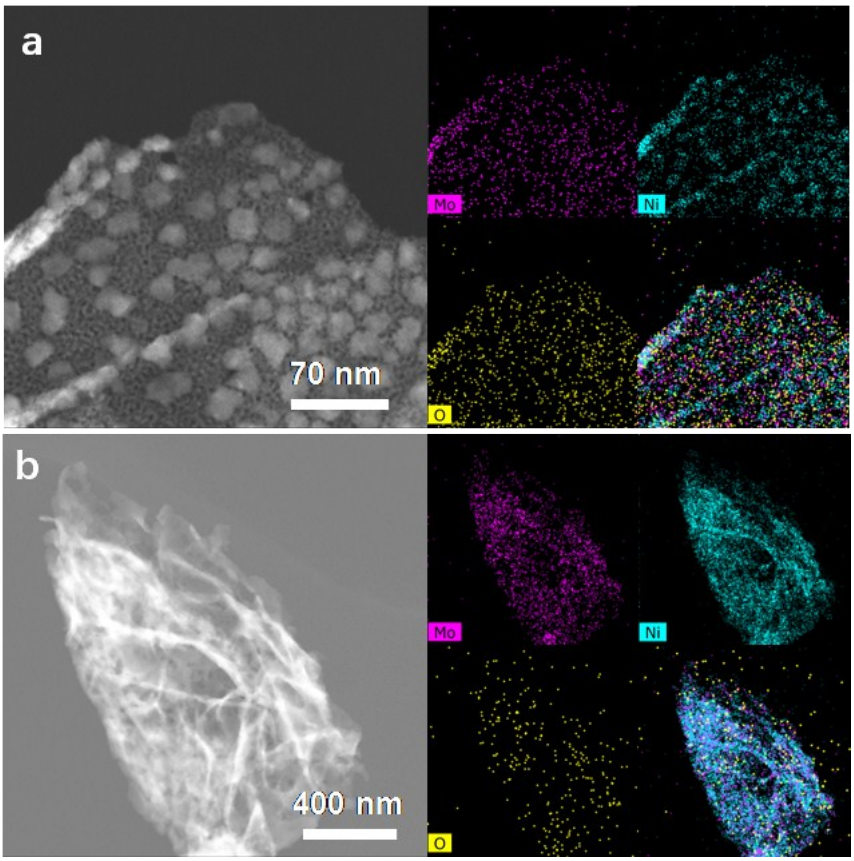

Figure S1. HAADF-STEM images and corresponding EDS mapping results of the samples annealed at 550 °C (a) and 700 °C (b).

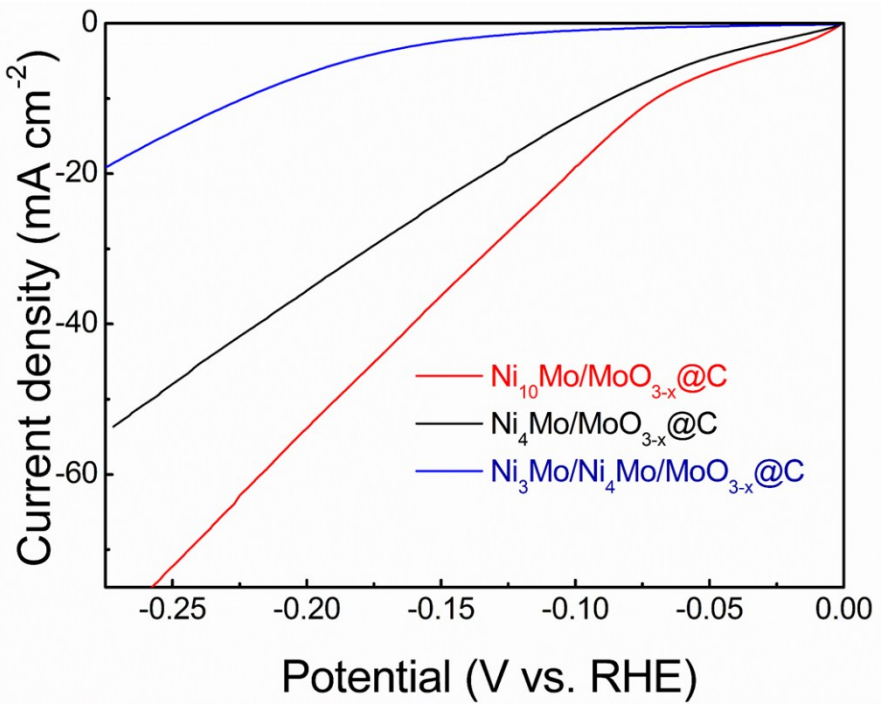

Figure S2. HER polarization curves of the Ni-Mo-O derived electrocatalysts supported on carbon paper.

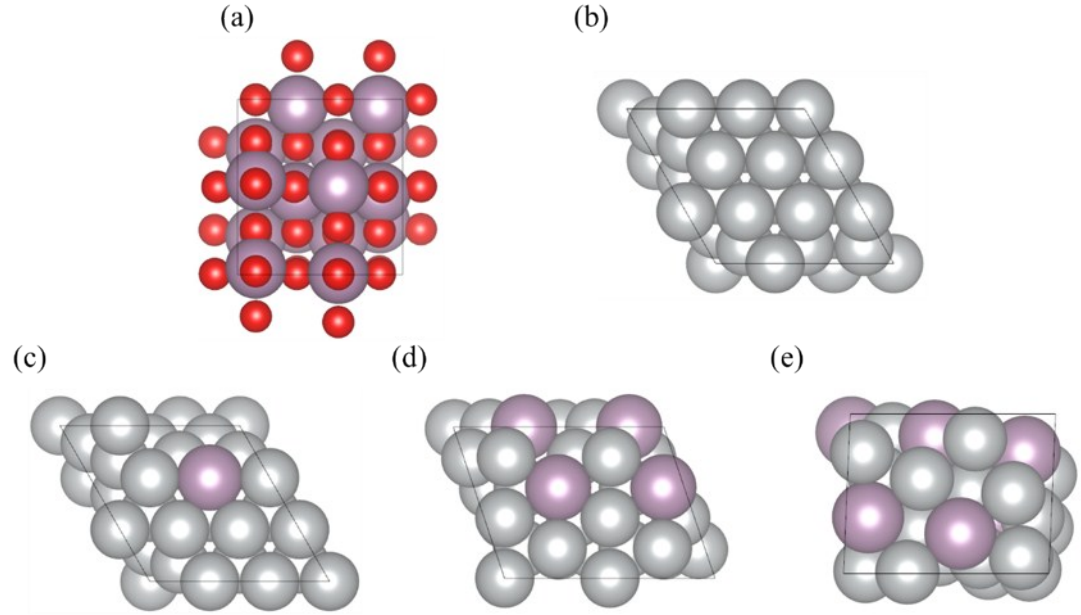

Figure S3. Top view of the models of (a) $MoO_3(010)$, (b) Ni(111), (c) $Ni_{10}Mo(111)$, (d) $Ni_4Mo(121)$, and (e) $Ni_3Mo(211)$. The light purple, silvery and red balls represent Mo, Ni, and O atoms, respectively.

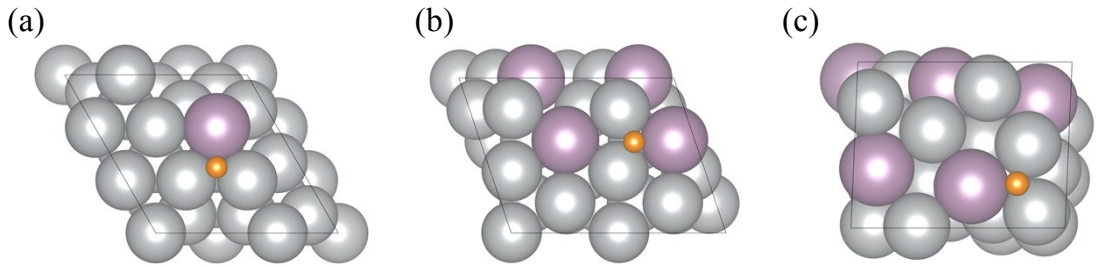

Figure S4. Adsorption site of H atom on (a) $Ni_{10}Mo(111)$, (b) $Ni_4Mo(121)$ and (c) $Ni_3Mo(211)$. The light purple, silvery and orange balls represent Mo, Ni, and H atoms, respectively.

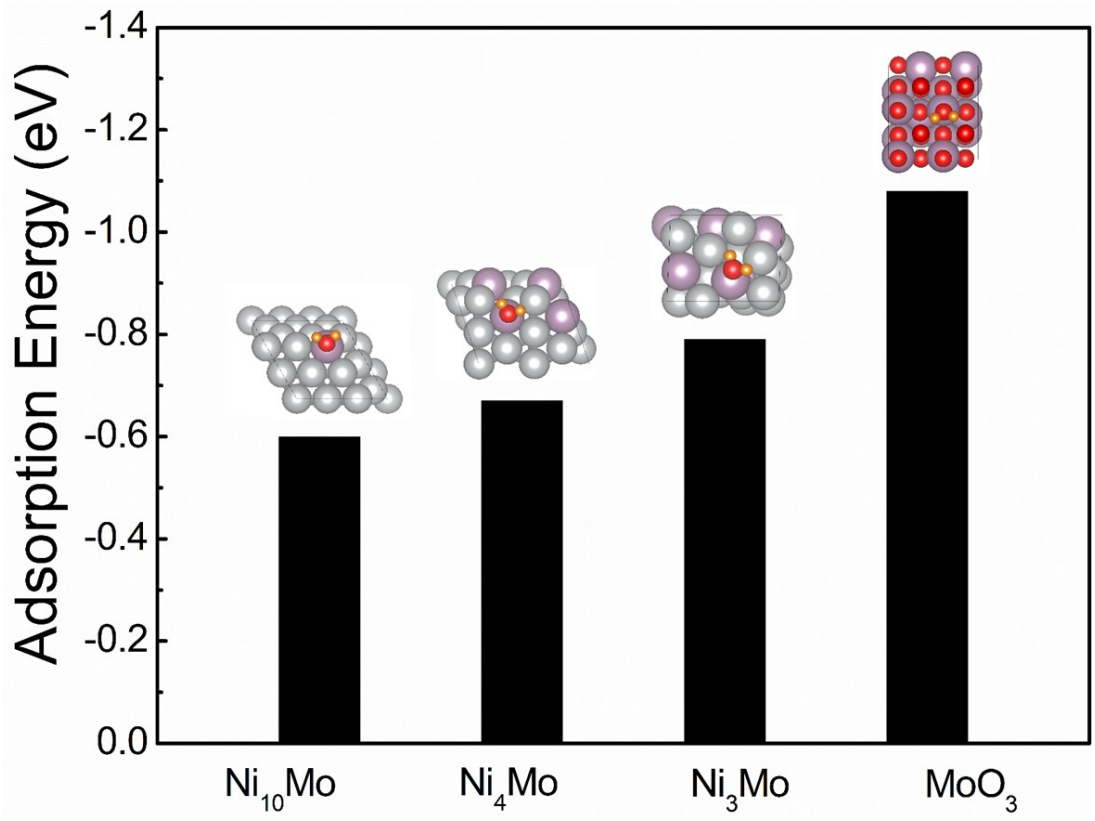

Figure S5. The calculated adsorption energies (ΔE_{ad}) of H_2O on $Ni_{10}Mo$, Ni_4Mo, Ni_3Mo and MoO_3 surfaces. The light purple, silvery, red and orange balls represent Mo, Ni, O and H atoms, respectively.

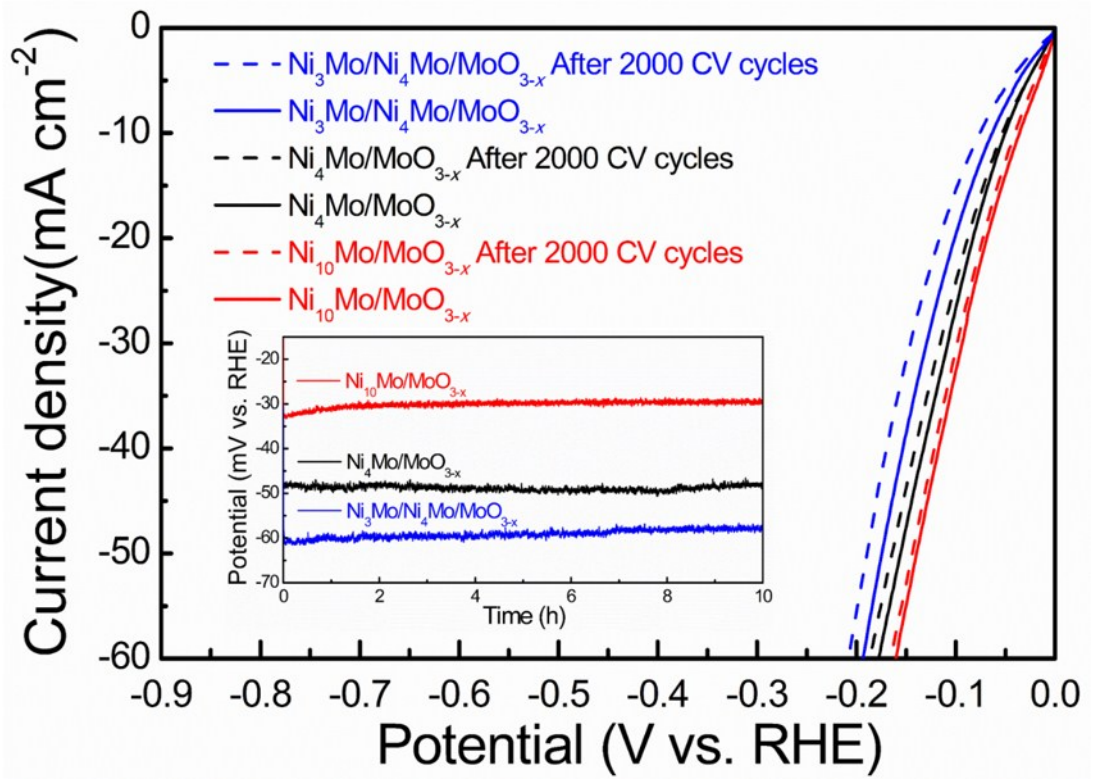

Figure S6. Polarization curves of the Ni-Mo-O derived electrocatalysts before and after 2000 cyclic voltammetry cycles, inset: Long-term stability tests of the Ni-Mo-O derived electrocatalysts at 10 mA cm^{-2}.

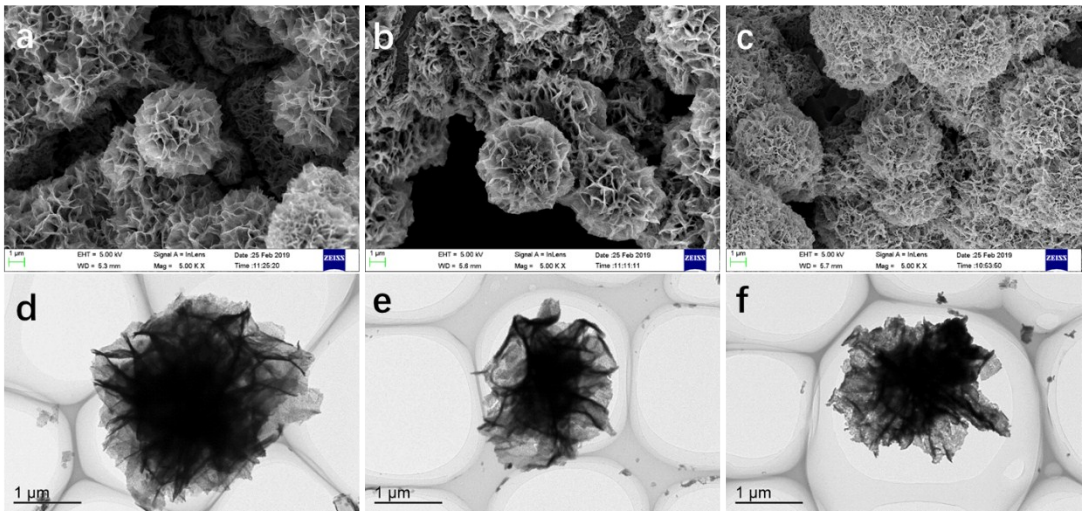

Figure S7. SEM images of the annealed samples treated at 380 ^{o}C (a), 550 ^{o}C (b), 700 ^{o}C (c) after long-term HER operations. TEM images of the annealed samples treated at 380 ^{o}C (d), 550 ^{o}C (e), 700 ^{o}C (f) after long-term HER operations.

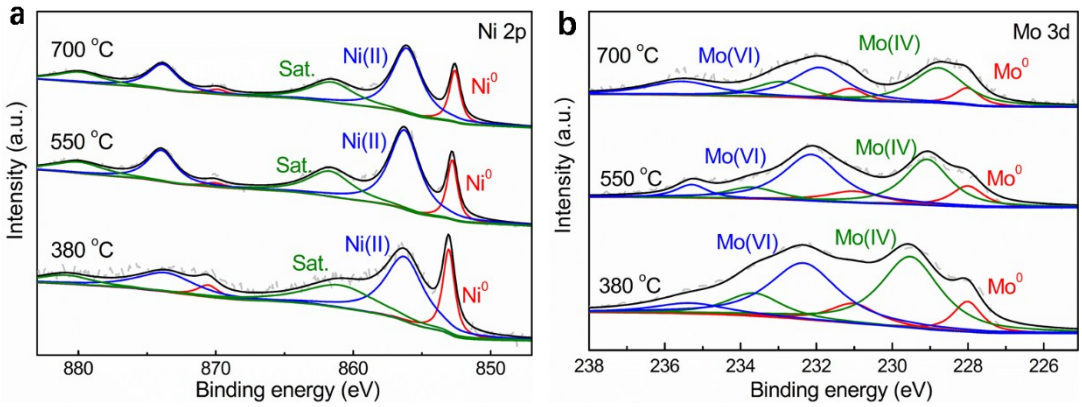

Figure S8. Ni 2p (a) and Mo 3d (b) XPS spectra of the annealed samples after long-term HER operations.

Notes and references

1 Y. Yoon, B. Yan and Y. Surendranath, *J. Am. Chem. Soc.*, 2018, **140**, 2397–2400.
2 G. Kresse and J. Furthmüller, *Phys. Rev. B*, 1996, **54**, 11169−11181.
3 J. Klimes, D. Bowler and A. Michaelides, *Phys. Rev. B*, 2011, **83**, 195131.
4 S. Dudarev, G. Botton, S. Savrasov, C. Humphreys and A. Sutton, *Phys. Rev. B*, 1998, **57**, 1505.
5 P. E. Blöchl, *Phys. Rev. B*, 1994, **50**, 17953−17979.
6 G. Kresse and D. Joubert, *Phys. Rev. B*, 1999, **54**, 1758−1775.
7 J. Neugebauer and M. Scheffler, *Phys. Rev. B*, 1992, **46**, 16067.
8 J. K. Nørskov, J. Rossmeisl, A. Logadottir and L. Lindqvist, *J. Phys. Chem. B*, 2004, **108**, 17886−17892.
9 V. Pallassana, M. Neurock, L. B. Hansen and J. K. Nørskov, *J. Chem. Phys.*, 2000, **112**, 5435−5439.
10 B. Hammer and J. K. Nørskov, *Adv. Catal.*, 2000, **45**, 71−129.